ISBN: 978-3-95450-225-7 ISSN: 2673-5571 doi:10.18429/JACoW-HB2021-MOP05

REDUCTION OF THE BEAM JITTER AT THE PIP2IT TEST ACCELERATOR*

A. Shemyakin†, G. Saewert, A. Saini, Fermilab, Batavia, IL 60510, USA

Abstract

Analysis of the beam position monitor (BPM) signals at the H- test linear accelerator PIP2IT showed that a large portion of the signals scatter comes from the beam jitter. BPM position measurements of the jitter modes were compared with beam orbit responses to perturbations excited by driving various beamline parameters in a low frequency sinusoidal manner. The main contributor to the jitter was found to be a low-frequency noise in the input reference to the ion source high voltage (HV) power supply. Filtering the HV power supply reference signal decreased the rms scatter in BPM readings by a factor of 2-3.

INTRODUCTION

The PIP-II Injector Test (PIP2IT) [1] was an H^- ion linac that was assembled in several stages in 2014-2021 to test critical elements of the front end of the PIP-II accelerator currently under development at Fermilab [2]. In its final configuration (Fig. 1), the PIP2IT consisted of a 30 kV, 15 mA H^- DC ion source, a 2 m long Low Energy Beam Transport (LEBT), a 2.1 MeV CW 162.5 MHz RFQ, a 10 m Medium Energy Beam Transport (MEBT), two cryomodules (HWR and SSR1) accelerating the beam up to 17 MeV, a High Energy Beam Transport (HEBT), and a beam dump.

Transverse focusing was provided by solenoids in the LEBT and cryomodules, and by quadrupole doublets and triplets in the MEBT and HEBT. Each doublet/triplet or solenoid (except in the LEBT) was accompanied by a BPM operating at 162.5 MHz.

The PIP2IT beam was operated in the pulse regime with 20 Hz repetition rate and the bunch population corresponding to the pulse current of 5 mA. The pulse duration varied up to 25 ms, but all measurements described in this paper were performed at 10 μs.

Soon after beginning of MEBT operation, it was observed that the pulse-to-pulse variation in the positions measured by BPMs significantly exceeded the expected electronics noise. The scatter was analysed, similar to what has been reported before (e.g. see Ref. [3]), by simultaneous recording of signals from all BPMs for tens of minutes and applying Singular Value Decomposition (SVD) to the resulting matrix. The scatter was dominated by a single mode. The ratio between the first and second eigenvalues was found to be about 10, and the components beyond the second eigenvalue were already at the noise floor [4].

The first spatial eigenvector was found to be a linear combination of the MEBT betatron modes starting from the RFQ exit. It clearly indicated that the BPM position scatter was dominated by the beam jitter originated upstream of the MEBT. Initial attempts to identify the source of the jitter by checking parameters readbacks in the ion source and LEBT were unsuccessful because of a high level of noise in the reading channels themselves.

While additional analysis [5] showed that the increase in projected emittances due to the jitter is small, the BPM readings scatter did negatively affect quality of measurements. Consequently, in the final run of PIP2IT additional efforts were made to find and correct the source of the jitter.

CHARACTERIZATION OF BEAM JITTER

An example of beam jitter characterization is shown in Fig. 2. In this measurement, the beam was propagating to the middle of the MEBT at the energy of 2.1 MeV, and beam positions, averaged over a pulse, were recorded by horizontal (X) and vertical (Y) channels of 7 BPMs for 500 seconds at 20 Hz pulse rate. The typical rms scatter was about 0.1 mm (Fig. 2a). The resulting (m=10000) x (n=14) matrix M was decomposed with SVD in MathCad into a product of three matrixes:

$$M = ULV^T, \quad (1)$$

where L is a diagonal $n \times n$ matrix populated with eigenvalues ordered in the descending order; U is an $m \times n$ matrix composed of temporal eigenvectors, and V is a $n \times n$ matrix of spatial eigenvectors.

As Fig. 2b shows, the 1st eigenvalue exceeded the 2nd by a factor of 6. The Fourier spectrum of the 1st temporal eigenvector (Fig. 2c) is composed mainly by low-frequency (< 4 Hz) components, with a prominent peak at 1.1 Hz. While this peak was not a dominant contributor to the rms jitter value, it was a convenient marker to match while looking for the noise source. To describe the spatial

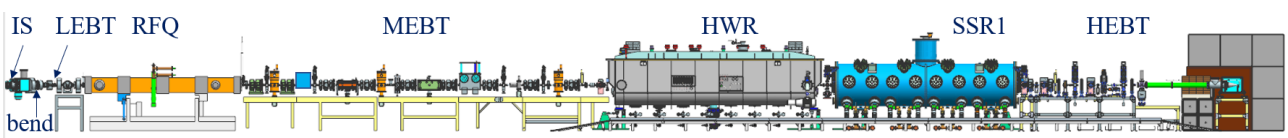

Figure 1: Side view of the PIP2IT.

* This manuscript has been authored by Fermi Research Alliance, LLC under Contract No. DE-AC02-07CH11359 with the U.S. Department of Energy, Office of Science, Office of High Energy Physics
† shemyakin@fnal.gov

ISBN: 978-3-95450-225-7 ISSN: 2673-5571 doi:10.18429/JACoW-HB2021-MOP05

eigenvector, it is compared with the simulated betatron motion.

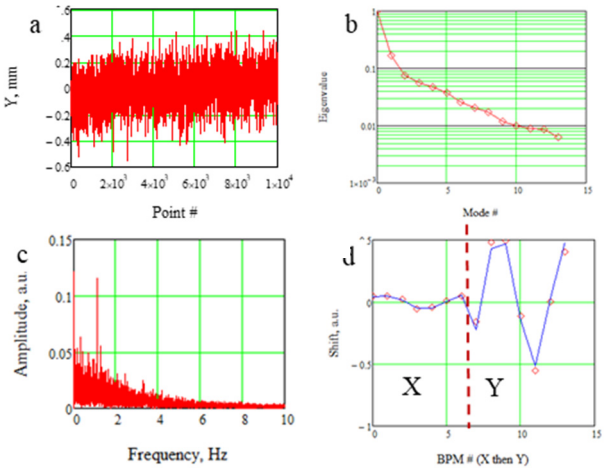

Figure 2: Example of jitter characterization. a- raw signal in Y channel of BPM #3, b- eigenvalues, c- temporal spectrum of the first mode. d- fitting of the 1st spatial eigenvector (red dots) to a sum of the betatron modes (blue line). The horizontal axis is the BPM channel number, first X and then Y channels.

First, four "base" trajectories are simulated using OptiM [6] code with the initial conditions at the exit of the RFQ, corresponding to a non-zero value (1 mm or 1 mrad) of only one degree of freedom (either offset or initial angle) in either horizontal or vertical plane. Any beam trajectory in the MEBT is a sum of these base trajectories with coefficients equal to the initial conditions (x_n, x_n', y_n, y_n'). Consequently, the set of initial conditions corresponding to the best fit of the spatial eigenvector (as in Fig. 2d) was used as a characteristic of the noise mode. To express all elements of such set in the same units, they were transformed to canonical variables using the simulated Twiss parameters $\alpha_x, \beta_x, \alpha_y, \beta_y$, thus forming the characteristic vector R_n:

$$R_n = \left(\frac{x_n}{\sqrt{\beta_x}}, \sqrt{\beta_x} x_n' + \frac{\alpha_x x_n}{\sqrt{\beta_x}}, \frac{y_n}{\sqrt{\beta_y}}, \sqrt{\beta_y} y_n' + \frac{\alpha_y y_n}{\sqrt{\beta_y}} \right). \quad (2)$$

A good fit in Fig. 2d indicates that the mode was indeed associated with beam motion and was originated upstream of the first BPM.

FINDING THE ORIGIN OF THE JITTER

Since no direct position measurements were available upstream of the MEBT, a different procedure was developed to search for the jitter origin. Responses of the beam orbit in the MEBT to various ion source and LEBT parameters were recorded. An orbit response was defined as a difference between BPM readings at nominal settings and with one of parameters (e.g. current of a dipole corrector in the LEBT) changed. Then, the resulting patterns were compared with the spatial distribution of the MEBT noise described in the previous section.

Initial measurements, performed in 2018, literally followed this orbit response definition. The difficulty with such measurements was their poor accuracy. At small parameter variations, contributions of the jitter and parameters drifts were significant as indicated by poor fits to the base trajectories. An increase in the number of pulses measured for each orbit did not significantly improve the actual scatter in the results. An explanation could be that the increased time between orbit measurements enhanced contribution of slow drifts. On the other hand, larger parameter variations resulted in non-linear orbit responses due to beam dynamics in the RFQ.

To resolve this issue, in 2021 the orbit responses were measured with an "oscillating trajectory" method, where a small amplitude sine wave variation was applied to the parameter value, and the Fourier component in the spectrum of all BPMs corresponding to the excitation frequency was recorded, with a proper normalization, as the response. The method was eventually implemented for all orbit response measurements at PIP2IT [7]. This technique applied in the NSLS-II ring had been discussed in Ref. [8]. Example of such measurement at PIP2IT is shown in Fig. 3.

$$\cos\theta_i = \frac{R_n \cdot R_i}{|R_n||R_i|}, \quad (3)$$

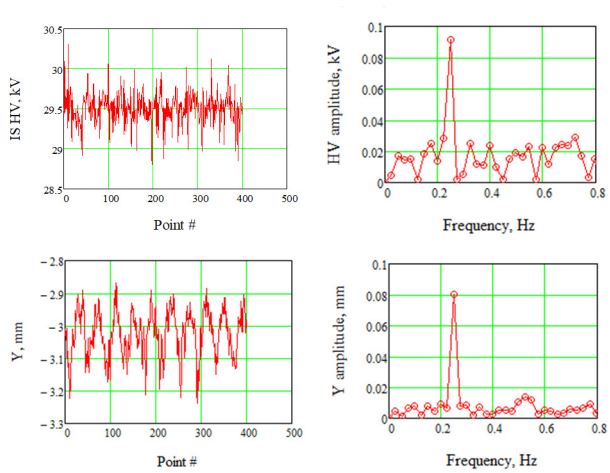

Figure 3: Example of orbit response measurement with oscillating trajectory: response of Y channel of the 1st BPM to excitation of the ion source high voltage at 0.25 Hz. 402 points are recorded at 10 Hz. Top row shows readings of IS HV, and the bottom row is the BPM. Left column presents the raw signals, and the right column is the relevant part of the Fourier spectra.

The recorded orbit response was fitted to the base trajectories, and the initial condition vector R_i was obtained for each tested parameter in the same manner as shown in Eq. (2).

The noise measurements were repeated at the same shift when the orbit responses were measured to ensure identical focusing. In this case, any trajectory is fully determined by its initial conditions, and initial condition vectors of similar trajectories should be colinear. Therefore, the angle θ_i between the orbit response and noise vectors was chosen as a measure of similarity, with the angle calculated as

ISBN: 978-3-95450-225-7 ISSN: 2673-5571 doi:10.18429/JACoW-HB2021-MOP05

$$\cos\theta_i = \frac{R_n \cdot R_i}{|R_n||R_i|}, \quad (3)$$

where dot represent the scalar product of the vectors.

The results for the 1st and 2nd modes are presented in Table 1 for excitation by the ion source high voltage (IS HV), 5 dipole correctors, LEBT bend, and LEBT chopper. Two measurements repeated at different amplitudes (with the corrector P:L10CYI and with the LEBT bend) show a reasonable reproducibility.

Table 1: Absolute Values of the Angle Between Noise and Orbit Response Vectors

	Mode 1	Mode 2
Ion Source HV	0.018	1.540
P:L00CXI	0.995	0.625
P:L00CXI	0.771	0.849
P:L10CXI	0.590	1.030
P:L10CYI	1.191	0.333
P:L10CYI	1.038	0.485
P:L20CXI	0.025	1.502
P:L20CYI	1.148	0.472
P:L30CXI	1.138	0.386
P:L30CYI	0.663	0.957
LEBT bend	0.366	1.254
LEBT bend	0.344	1.276
LEBT chopper	1.235	0.597

Two excitations, highlighted in the table, with the IS HV and P:L20CXI (the horizontal corrector in the second solenoid), both produce the angles close to zero. Their spatial distributions fitted to the first jitter mode are shown in Fig. 4.

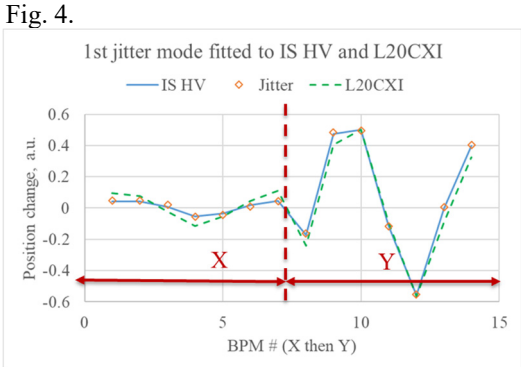

Figure 4: Comparison of the first spatial mode of the beam jitter in the MEBT (orange diamonds) with the best fits of responses to excitation by IS HV (solid line) and corrector P:L20CXI (dashed line).

To explain the observed beam jitter using the fit shown in Fig. 4, the noise in the P:L20CXI corrector current needed to be by about 8 times higher than the noise value measured in its readback. Therefore, the corrector was ruled out as the primary source of the jitter.

On the other hand, the fit assuming that the jitter was originated in the IS HV required 56 V rms noise (out of 30 kV DC), while its readback delivered the noise with 200 V rms.

The presented results were considered conclusive enough to justify additional efforts of investigating the ion source high voltage stability.

Note that instead of the described procedure of comparing the initial vectors corresponding to the noise and the tested component with Eq. (3), initially we directly fitted the measured orbit responses to the noise spatial vector as it was done for Fig. 4. In this approach, the figure of merit was the rms error of fitting. Applying this procedure to the measurements used in Table 1 eventually gave the same result, pointing to IS HV as the jitter source. However, introduction of the intermediate step of fitting to the base trajectories helped to eliminate bad measurement sets and appeared to make the procedure more reliable and accurate.

REDUCTION OF THE JITTER

Following the conclusion derived in the previous section, a commercial 50 kV resistive divider was installed to monitor the 30 kV DC IS HV power supply (PS) output. This signal was buffered and isolated from the instrumentation ground to eliminate any common mode noise that might be between the PS and instrumentation. A low frequency spectrum analyzer readily showed the frequencies of interest, and particularly the 1.1 Hz line (Fig. 5 left).

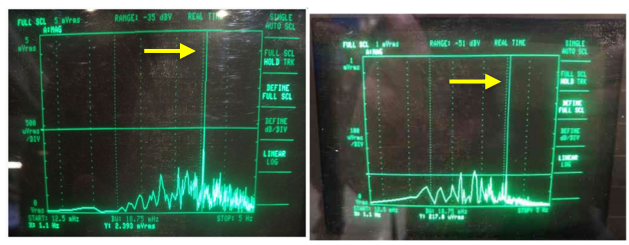

Figure 5: Screenshots of the low frequency spectrum analyzer showing the signal from the resistive divider before (left) and after (right) installation of the filter. The arrows indicate the 1.1 Hz marker. The vertical scale is 5 mV in the left plot and 1 mV on the right.

This analyzer was an HP 3561A Dynamic Signal Analyzer with 0.125 mHz to 100 kHz bandwidth. It was used with AC coupling that suppressed the signal below ~0.1 Hz.

The ripple specified for the IS HV PS, Glassman LT40N50, is small, < 12 V rms [9]. Therefore, we suspected that the noise could be caused by the reference DAC signal and/or common mode noise between the DAC and PS. The same spectrum analyzer was used to measure the ground signals between the 30 kV PS and the DAC reference chassis and showed the same noise spectrum at about the expected amplitude. Hence, a low-pass R/C filter having a cut-off frequency pole at 0.12 Hz was installed at the PS reference input, attenuating both the common mode and single-ended noise arriving over the long cable from the DAC reference.

ISBN: 978-3-95450-225-7 ISSN: 2673-5571 doi:10.18429/JACoW-HB2021-MOP05

The measurements of the HV output spectrum, repeated after installation of the filter, showed a significant decrease of the noise (Fig. 5 right). For example, the rms amplitude of the characteristic 1.1 Hz line decreased from 2.4 to 0.22 mV.

The measurements of the BPM scatter were repeated for same transverse focusing before and after installation of the filter with the beam propagated through the entire PIP2IT without acceleration in the cryomodules. Comparison of the rms scatter in each BPM channel is shown in Fig. 6. After installation of the filter, the rms scatter, averaged over all BPMs, decreased by 2.5 times in X and by 3.1 times in Y.

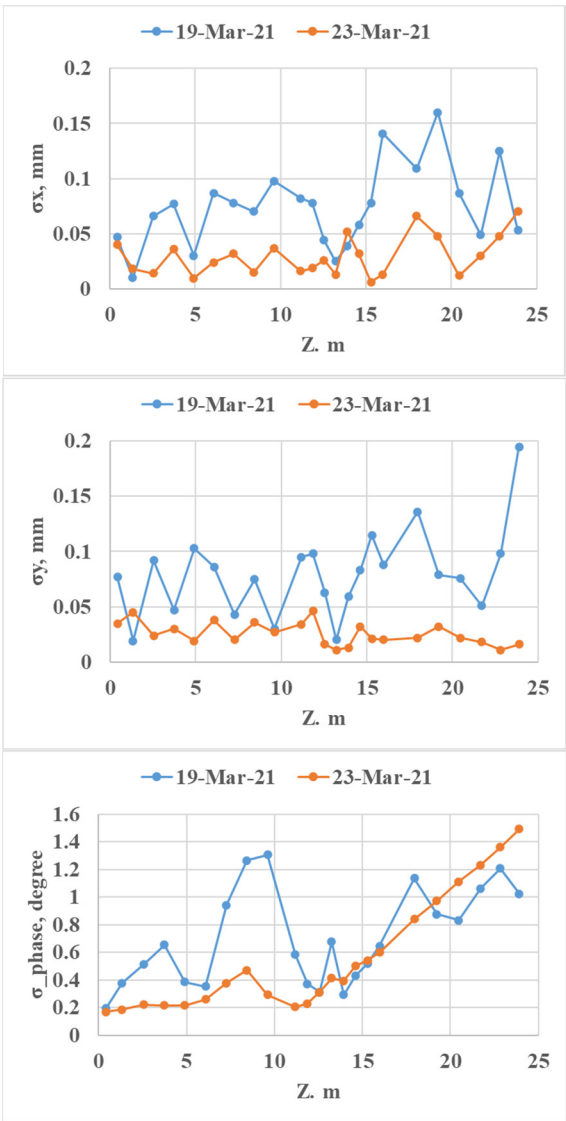

Figure 6: Comparison of the scatter in BPM readings before (marked 19-Mar-21) and after (23-Mar-21) installation of the IS HV PS reference input filter. Beam energy was 2.1 MeV. 5000 points recorded at 20 Hz were analyzed in each case. The top, middle, and bottom plots show the rms scatter for each BPM in horizontal vertical, and longitudinal (phase) planes, correspondingly. The phases are expressed in units of degrees of 162.5 MHz.

The scatter in the phases recorded by BPMs decreased significantly as well, as shown in Fig. 6 bottom plot. A numerical comparison of all BPM readings is not applicable since the field amplitudes in the last two bunching cavities were slightly different between two measurements. While it doesn't affect noticeably the transverse dynamics, the energy jitter in the drift space downstream of the MEBT strongly depends on specific bunching cavities' settings. Inside the MEBT (Z <10 m), the average rms scatter decreased by a factor of 2.5.

Since the decrease of the BPM phase scatter was not originally expected, the phase signals in the data sets used for Fig. 6 were analysed in more detail. The BPM phase signals before installation of the IS HV PS filter showed the frequency spectrum very similar to the one shown in Fig. 2c for the transverse motion, with the same characteristic 1.1 Hz line. Analysis of the first SVD spatial mode indicated that it corresponded to the energy jitter at the exit of the RFQ with rms amplitude of 0.2 keV.

After the filter installation, the 1.1 Hz line disappeared in all BPM signals. The remaining noise was confined to frequencies below 0.2 Hz. The eigenvalues of the first modes were comparable, which indicated that the beam jitter was indistinguishable at the measurement noise.

Response of the BPMs to excitation of the IS HV (before installation of the filter) was recorded as well (Fig. 7). Since the measurement was made again at different settings of the bunching cavities, direct fitting to the beam jitter was not possible. However, conditions at the RFQ exit calculated from the Fig. 7 data agreed with observations in the beam jitter: the response in the initial phase was close to zero, and variation of energy was 3.8 times higher than variation of the IS HV.

We conclude that before installation of the filter a dominant portion of the BPM phase scatter was also related to the noise of IS HV.

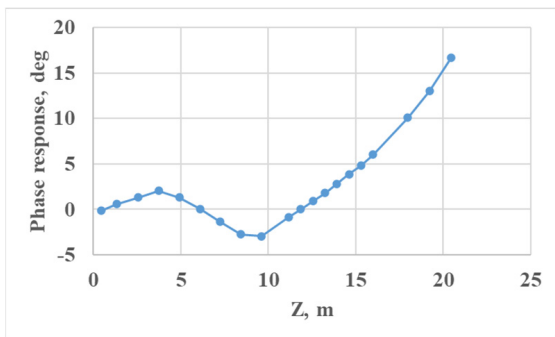

Figure 7: Response of BPM phases to oscillation of the IS HV with 0.2 kV amplitude and 0.125 Hz frequency. 802 points were recorded at 5 Hz. Beam energy was 2.1 MeV.

CONCLUSION

The scatter in BPM readings at PIP2IT was analysed with SVD and found to be dominated by the beam jitter. To find the source of the jitter, responses of the orbit in the MEBT to variation of parameters in the LEBT and the ion source were measured by applying a small-amplitude si-

ISBN: 978-3-95450-225-7 ISSN: 2673-5571 doi:10.18429/JACoW-HB2021-MOP05

nusoidal variation to each parameter and recording the corresponding line in the BPM spectra. Comparison of these orbit responses with the jitter spatial pattern determined that the source of the jitter was the ion source high voltage noise at the level of about 60 V rms. The observation was supported by direct measurements of the high voltage signal. Installation of the low-pass filter at the HV power supply reference signal decreased the rms scatter in BPM position readings by a factor of 2-3. The scatter in BPM phase readings in the MEBT decreased as well by a similar factor.

ACKNOWLEDGEMENTS

Authors are thankful to the entire PIP2IT team for assistance with the measurements. All data acquisition programs were written by W. Marsh. Discussions with L. Prost and C. Jensen helped to identify the HV power supply reference signal as a likely source of the noise. Support of N. Eddy with BPM measurements is appreciated.

REFERENCES

[1] P. Derwent *et al.*, "PIP-II Injector Test: Challenges and Status", in *Proc. 28th Linear Accelerator Conf. (LINAC'16)*, East Lansing, MI, USA, Sep. 2016, pp. 641-645. doi:10.18429/JACoW-LINAC2016-WE1A01

[2] L. Merminga *et al.*, "The Proton Improvement Plan-II (PIP-II): Design, physics, and technology advances", invited submission to Phys. Rev. Accel. Beams (in preparation), 2021.

[3] J. Irwin *et al.*, "Model-independent analysis with BPM correlation matrices", in *Proc. EPAC'98*, Stockholm, Sweden, Jun. 1998, pp. 1644-1646.

[4] A. Shemyakin *et al.,* "Experimental study of beam dynamics in the PIP-II MEBT prototype", in *Proc. of HB'18*, Daejeon, Korea, Jun. 2018, pp. 54-59. doi:10.18429/JACoW-HB2018-MOP1WB03

[5] A. Saini *et al.*, "Beam tests of the PIP-II Injector Test Radio Frequency Quadrupole", *Nucl. Instrum. Methods Phys. Res., Sect. A,* vol. 978, p. 164368, 2020. doi:10.1016/j.nima.2020.164368

[6] OptiM, http://home.fnal.gov/~ostiguy/OptiM/.

[7] A. Shemyakin, "Orbit response measurements with oscillating trajectories", Fermilab, USA, FERMILAB-TM- 2763-AD, 2021, https://arxiv.org/abs/2109.11589

[8] X. Yang, V. Smaluk, L. H. Yu, Y. Tian, and K. Ha, "Fast and precise technique for magnet lattice correction via sine-wave excitation of fast correctors", *Phys. Rev. Accel. Beams,* vol. 20, p. 054001, 2017. doi:10.1103/PhysRevAccelBeams.20.054001

[9] Glassman catalog, https://www.vicomtrade.cz/pdf/glassman-catalog.pdf